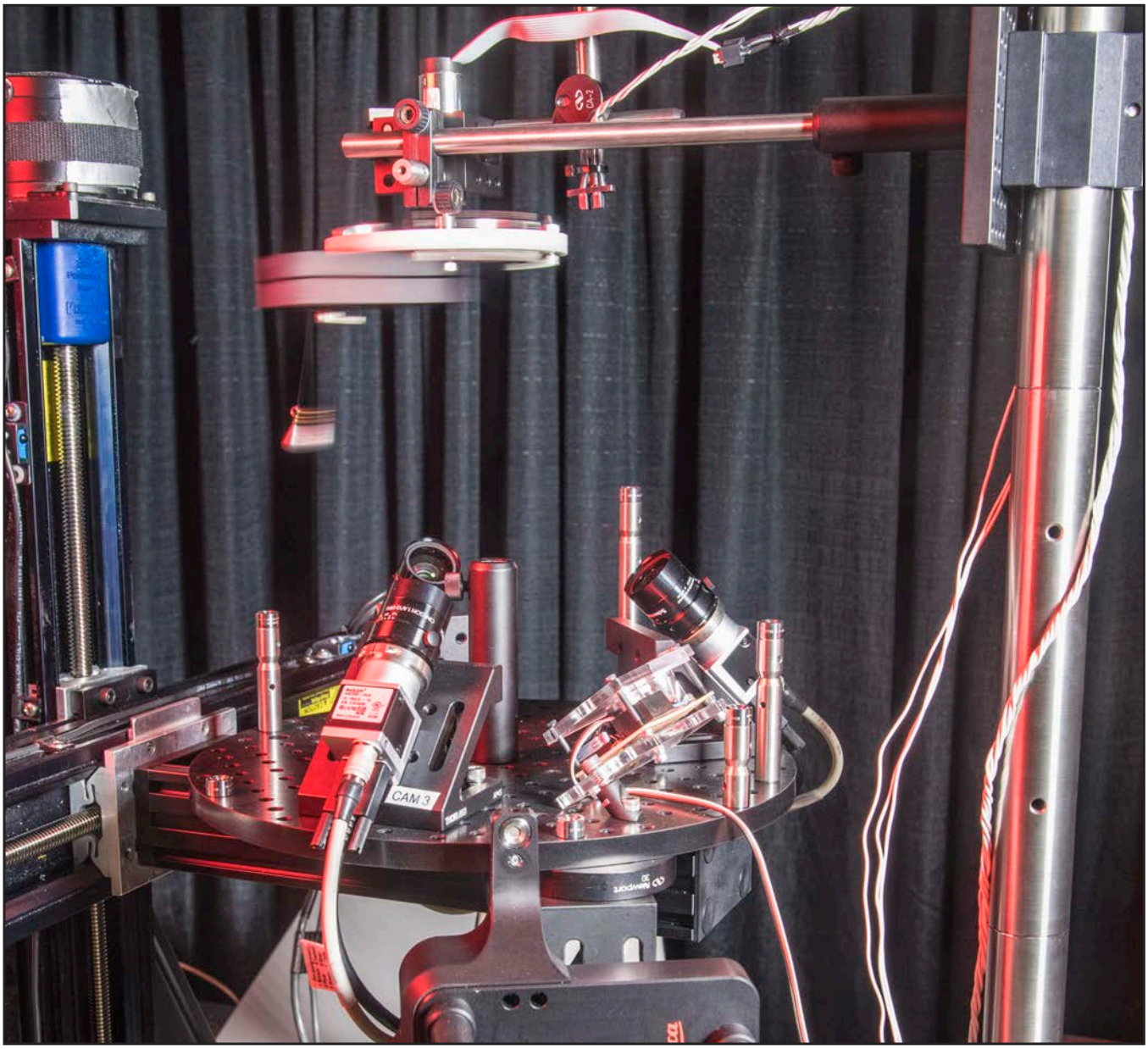

Freezing Time: Dynamic Laser Tracker Measurements With the Pixel Probe Using Temporal Aliasing

by Joshua A. Gordon, NIST, and
Steven S. Borenstein, Colorado School of Mines

In this article, we present a noncontact technique for measuring objects in motion with a laser tracker without need of the laser tracker following the object. This method allows the dynamic state of an object to be measured while, to the laser tracker, the object appears to be stationary. Through temporal aliasing, this technique decomposes the dynamic frame of an object into an instantaneous stationary frame of reference with respect to the laser tracker. The Pixel Probe and laser tracker are used to demonstrate this method. The frame rate of the three cameras in the Pixel Probe are adjusted to selectively alias the motion of an object into a stationary frame of reference. By triggering the cameras in

the Pixel Probe at an appropriate frequency, the object in motion appears stationary to the Pixel Probe and therefore to the laser tracker as well. This allows spatial metrology to be performed on a dynamic object without the need to operate the laser tracker dynamically.

We present measurements of rigid optical targets under both stationary and dynamic conditions. The dimensions of the rigid targets should be the same for both the static and dynamic cases; therefore, these targets provide a controlled experiment. These data are used to validate this technique by providing a direct comparison of accuracy between the use of aliasing with the Pixel Probe to the stationary case. Measurements for a nonrigid body are also made where a mass at the end of a string is constantly rotated at several frequencies. The dynamic 3D motion of the rotating mass is measured and compared to the predictions of Newtonian mechanics. We show that through the purely spatial measurements made with this technique, the rotation frequency of the mass can be determined to less than 1 percent. Furthermore, this technique may enable 3D characterization and calibration of a laser tracker under dynamic conditions, as the laser tracker motion can be decoupled from the calibration target motion, thus allowing direct determination of the dynamic performance of the laser tracker.

INTRODUCTION

In this article we describe a noncontact technique for measuring moving objects with a laser tracker in which the laser tracker need not actually follow the object. A new, simple, and effective noncontact spatial metrology probe, the Pixel Probe, has previously been presented.[1] The Pixel Probe is constructed from three digital focal plane arrays (FPA) and imaging lenses, and it operates by projecting the image of a single pixel from each of three digital cameras to a common point in space. This point is simultaneously linked to each pixel and to the laser tracker coordinate system via a calibration process, also previously described.[1] The combination of the three pixel images in effect forms a virtual spatial metrology probe and allows noncontact measurements to be made with a laser tracker. In the current configuration, spatial resolution of approximately 25 μm is achieved, which can be improved through scaling of the optical system magnification. The use of digital cameras allows unique spatial and temporal operational modes with the Pixel Probe. For example, patterns in images which have been derived using feature-recognition algorithms can be measured directly with a laser tracker. An example of this is using an ellipse-finding algorithm in the Pixel Probe images to locate the 3D location of the center of a hole with the laser tracker. Furthermore, the video-capture ability of the cameras also allows spatial and temporal information to be combined so that dynamic measurements can be made.

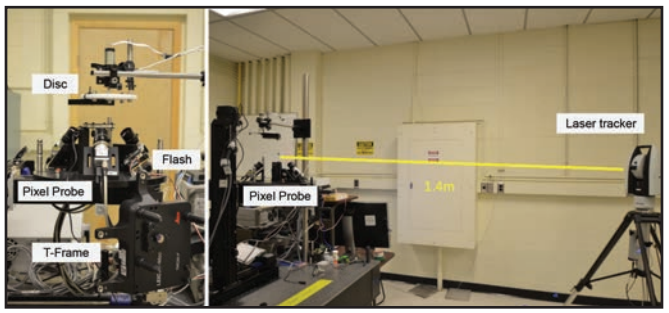

Figure 1. Experimental setup: at left, Pixel Probe with T-Frame, rotating disc, and flash; at right, laser tracker at a distance of 1.4 m from the Pixel Probe during experiments

More specifically, moving objects can be measured using a laser tracker without the laser tracker having to move with the object. To achieve this, the frame rate of the three cameras in the Pixel Probe are adjusted to purposely alias the motion of the object. In this way, the object appears stationary in the Pixel Probe images and therefore also appears stationary to the laser tracker. This article presents proof-of-concept measurements showing the ability to measure the dimensions of moving objects rotating at fixed frequencies with the laser tracker operating in a stationary mode.

Two cases are explored. In the first, rigid optical targets are measured to provide a validation and a comparison of this technique between stationary and dynamic measurements. As these rigid targets should not change shape (under the forces experienced from the rotation frequencies used), both stationary and dynamic measurements should provide the same results if this technique is sound.

The second case measures a body that is intended to change spatially under different rotational forces. A fishing weight suspended from a string was rotated at several frequencies and its displacement in three dimensions from stationary was measured. The three-dimensional displacements of the weight for several rotational frequencies are measured. The rotational frequencies are then determined using the purely spatial measurements and Newton's equations, and are then compared to the known input rotation frequencies. Again, if this approach is sound for measuring a dynamically changing object, then the rotation frequencies determined from the Pixel Probe/laser tracker measured displacements should be the same as the known input rotation frequency.

EXPERIMENT

Setup

The experimental setup can be seen in figure 1. The Pixel Probe is attached to a three-axis motion stage and is set to view a rotating disc to which sample targets were mounted during measurement. The disc was constructed out of white diffuse plastic, which provided consistent near-Lambertian background lighting of targets. The three cameras for the Pixel Probe were constructed from 2,592 pixel × 1,944 pixel complementary metal oxide semiconductor (CMOS) FPAs and 12.5 mm focal-length low-distortion machine vision lenses. Instead of a constellation of 0.5-in. spherically mounted retroreflectors (SMRs) as used previously,[1] a six degree of freedom (6DOF) laser tracker, the Leica T-Frame from Hexagon Manufacturing Intelligence of North Kingstown, Rhode Island, was used to generate the reference frame of the Pixel Probe and link the three pixels to the

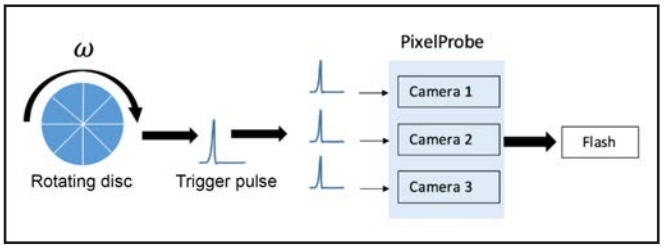

Figure 2. Triggering flow diagram: a pulse generated by the optical interrupt attached to the rotating disc is distributed to all three cameras; Camera 2 then initiates the flash

coordinate system. The use of the T-Frame made for more rapid measurements because the location of the three pixels could be traced with the laser tracker in real time rather than derived from the SMR constellation. Spatial metrology software was used to collect data from the laser tracker. The laser tracker was placed approximately 1.4 m away from the center of the spinning disc, which was limited due to laboratory space.

Temporal aliasing

For the targets attached to the spinning disc to appear stationary, the correct frame rate of the cameras needed to be achieved such that the rotational frequency was aliased to a frequency of zero. For these proof-of-concept experiments, a closed-loop scheme was used to trigger the cameras. In manipulating the sample motion via camera frame rate, space-frequency and position-phase relationships obeyed through Fourier theory[2] allow both the apparent rotation frequency as well as apparent position of the targets to be manipulated via camera triggering. By adjusting the frame rate (frequency) of the cameras to match the rotational frequency of the spinning disc, the target motion could be made to appear stationary. Similarly, by adjusting the trigger delay (phase), the position of the target could be adjusted and centered in the field of view of the Pixel Probe. A flow diagram for the triggering scheme can be seen in Figure 2.

With the target appearing stationary, the laser tracker could be used to perform measurements just as if the targets were actually stationary. The shutter mode of the FPA also plays a role in how complete the motion of an object can be aliased.

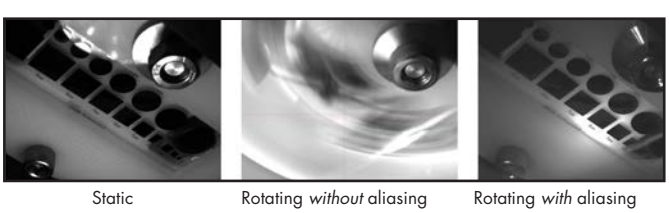

Figure 3. A visual comparison of the shape target under static conditions (left), rotation without aliasing (center), and rotation with aliasing (right); the shapes in these images appear the same for the static and aliased cases, and the central region appears brighter in the aliased image due to the more concentrated illumination of the flash

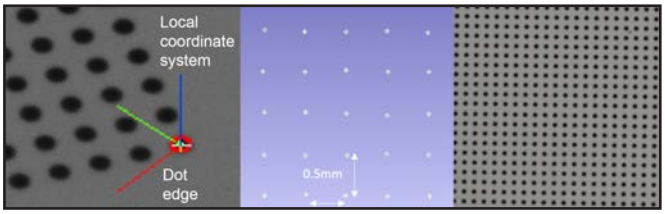

Figure 4. Dot grid target: left, centroid finding of dot center from edge detection, with the perimeter of the dot shown by the red ring, and the local coordinate system of the Pixel Probe (which exists in the laser tacker reference frame) shown as well; middle, data points for the 5 x 5 dot grid; right, photo of the grid target with 0.25-mm diameter dots spaced 0.5 mm apart on a regular square grid

The cameras used were limited to a rolling shutter operation as opposed to a global shutter. With a global shutter, the exposure start time and readout are the same for all rows of pixels, which limits image smear. In a rolling shutter mode each row of pixels has different exposure start times and readout times, which can smear the image. To negate the image smear an "effective global shutter" was created by specifying a time window within each shutter sequence during which an external flash is implemented. The flash duration is used to define the effective global frame capture period, which acts like an electronic global shutter. A visual comparison of images taken while the target was stationary, under rotation without aliasing, and under rotation with aliasing, can be seen in figure 3.

MEASUREMENT RESULTS

Rigid targets

Two rigid targets fabricated from optically flat glass plates 1.5-mm thick with shapes patterned from electron-beam-etched chrome were used for the measurement process. A grid target consisting of 250 μm diameter dots spaced 500 μm apart and a target consisting of square and circle shapes ranging in size from 0.5 mm to 10 mm were used. All shape dimensions are known to within ±2.5 μm per manufacturer specifications. The rigid targets can be seen in figures 4 and 5. The targets were measured while rotating and then while stationary. Although these targets are planar, the measurements obtained are fully 3D so that the shapes and the plane they lie in are known in an absolute sense in the laser tracker coordinate system.

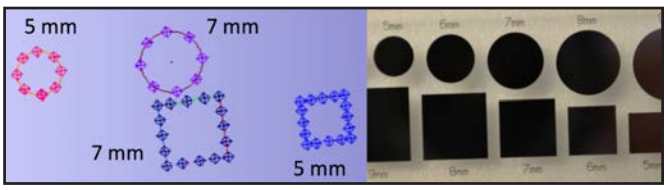

Figure 5. Circle and square shapes: left, nominally equispaced data points and fitted geometries are shown; right, actual shape target

Spacing (mm)	Mean (mm)			Standard deviation (mm)	
	Static	Dynamic	Δ Mean	Static	Dynamic
0.5	0.501	0.501	8.605E-05	0.014	0.010
1	1.000	1.003	3.206E-03	0.013	0.012
1.5	1.502	1.505	3.376E-03	0.011	0.011
2	1.999	2.006	6.386E-03	0.014	0.013
2.5	2.501	2.508	6.984E-03	0.020	0.017

Figure 6. Table show 5 × 5 dot grid center-to-center spacing

A rotation frequency of 0.25 Hz was used for the rigid target measurements, which was limited by the motor speed and not the camera frame rate. In principle, higher frequency movement could be measured by using high-speed cameras. The center-to-center spacing of a 5 × 5 grid of the dots was measured. The center of each dot was found by using the centroiding mode of the Pixel Probe.[1] In this mode the perimeter of each dot is found through a machine vision edge-detection process. An ellipse is then fit to the perimeter and the center of the ellipse is taken as the center of the dot, which can be seen in figure 4. The distances along the orthogonal directions of the grid for all pairs of dot center separations (from 0.5 mm to 2.5 mm) were measured. The mean and standard deviation for all center-to-center spacing

Square size	Static (mm)		Dynamic (mm)		Delta (mm)	
	S1 to S3	S2 to S4	S1 to S3	S2 to S4	D (S1 to S3)	D (S2 to S4)
5 mm	5.000	5.017	4.999	5.005	0.001	0.012
7 mm	7.015	7.011	7.003	7.001	0.013	0.010

Figure 7. Table showing rigid target measurement results, squares

Circle diameter	Static (mm)	Dynamic (mm)	Delta (mm)
5 mm	5.015	5.011	0.004
7 mm	7.001	7.018	0.017

Figure 8. Table showing rigid target measurement results, circles

pairs were then calculated. These data can be seen in the table in figure 6. The difference in the means for all spacings between the static and dynamic cases are below 10 μm with standard deviations <20 μm, which is consistent with the inherent uncertainty of the laser tracker. Circle and square shapes of 5 mm and 7 mm were also measured under the same conditions as seen in figure 5. Eight nominally equally spaced measurements were made around the perimeter of each circle and five measurements were made around the perimeter of each square. A circle fit was then calculated to

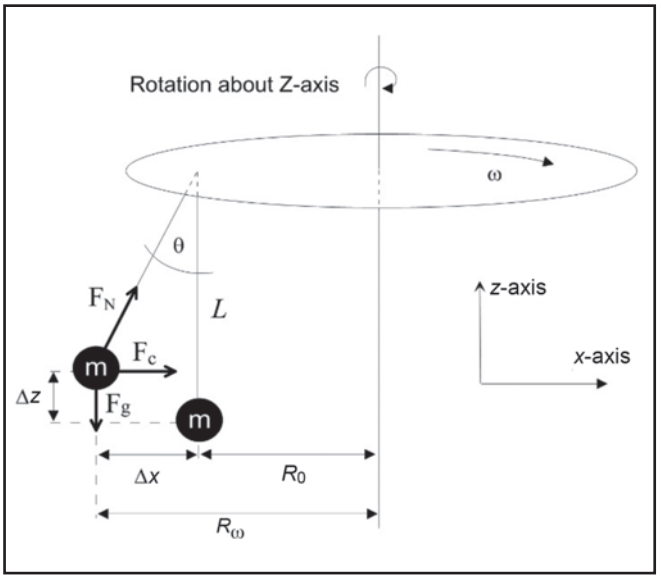

Figure 9. Mass "m" suspended from a disc rotating about the z-axis; centripetal F_c, and gravitational F_g forces are balanced by the normal force F_N of the string of length L, and for a given rotation frequency ω the orbital radius increases from the static radius R_o by an amount Δx, and the orbital plane is displaced by an amount Δz .

determine the radius. For the squares, lines were fit to all four sides (S1, S2, S3, S4) and the distances between adjacent sides (S1-to-S3, S2-to-S4) were calculated to determine the size. A comparison of measurement results between the stationary and dynamic cases for the squares and circles can be seen in the tables in figure 7 and 8, respectively. Results show errors better than 20 μm in all cases, which again are within the laser tracker uncertainty. These results suggest that measurement accuracy is not significantly degraded from the use of aliasing.

Dynamic target

To demonstrate the ability to fully characterize a dynamic system, a target that changes position in all three dimensions (*X, Y*, and *Z*) for different rotation frequencies was chosen. For this, a mass *m* rotating at a constant frequency was suspended a distance *L* from the disc by a string. While rotating, the normal force F_N exerted on the mass by the string must cancel the combined forces of gravity F_g and the centripetal force F_c, which results from the rotation. Therefore, the orbital radius of the mass will change as the frequency of rotation changes. A diagram depicting this can be seen in figure 9. While stationary, the mass occupies an orbital radius of R_0. As the disc rotates at a frequency of $\omega=2\pi f$ (where *f* is in units of Hz), the mass will be displaced by distances Δx, Δz in the *x* and *z* directions, creating an angle θ from the static position and occupying a new orbital radius of R_ω. Using Newton's equations for uniform circular motion an expression can be derived for what the rotation frequency should be based on measurements of *L*, Δx, Δz, and R_ω. Given the equation for centripetal force,[3]

$$F_c = m\omega^2 R_\omega \qquad \text{(Equation 1)}$$

and equating total horizontal forces we can write,

$$m\,\omega^2\,R_\omega = mg \cdot Tan(\theta) \qquad \text{(Equation 2)}$$

where $g = 9.8 m/s^2$ is the gravitational acceleration constant, it can be shown that (as seen in figure 9),

$$Tan(\theta) = \frac{\Delta x}{L-\Delta z} = \frac{(2\pi f)^2 R_\omega}{g} \qquad \text{(Equation 3)}$$

and therefore the rotation frequency is given by,

$$f = \sqrt{\left(\frac{\Delta x}{L-\Delta z}\right)\frac{g}{4\pi^2 R_\omega}} \qquad \text{(Equation 4)}$$

The mass used was a teardrop-shaped fishing weight which had a circular opening at the larger end and is seen in figure 10. The ellipse centroid finding mode of the Pixel Probe was used to measure the position of the center of this circular opening. The centroid-finding process is also seen in figure 10. Equation 4 was used to calculate the rotation frequency *f* from the measurements. For these calculations, the center of the opening was taken as the center of mass of the weight, which is close to the actual center of mass. Even though this location is not at the exact center of mass location, it provides a very good estimate for these proof-of-concept measurements as we show below.

The calculated frequencies were then compared to the known input frequencies. The table in figure 11 shows the experimental parameters and calculated frequencies. The differences between the actual frequency values and those determined from measurement were <0.01 Hz at all frequencies except the highest frequency at 0.85 Hz. This may be due to the fact that in equation 4, *f* becomes more sensitive to errors in the value of *L*. Therefore, the small error of knowing the exact distance the center of mass is from the disc becomes more significant. Furthermore, at 0.85 Hz the weight was observed to take on higher modes of movement and locally precess, creating a spread of values in Δx and Δz within the local precessing orbit. This may also account for the larger error at this frequency. As measuring higher-order movement

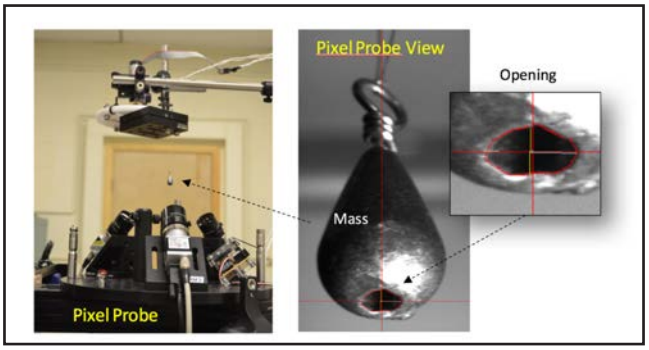

Figure 10. Left, setup for measuring the rotating mass; right, teardrop-shaped mass; crosshairs define the center of the opening at the end of the mass that was found using the Pixel Probe centroiding algorithm; inset, red highlighted edge pixels were used to find the centroid of the opening

f(Hz) Actual	*f*(Hz) Experiment	Δ*f* (Hz)	Δx (mm)	Δz (mm)	Rω (mm)	L (mm)
0	0	0	0	0	80.105	83.241
0.5	0.5015	0.00150	7.330	0.462	87.435	83.241
0.65	0.6523	0.0023	13.037	1.541	93.142	83.241
0.735	0.7379	0.0029	17.284	2.282	97.389	83.241
0.85	0.8307	0.0193	22.986	2.981	103.091	83.241

Figure 11. Table showing experimental parameters for rotating mass

was out of scope of this proof-of-concept experiment, future work will aim to expand the measurement capability of this technique to be able to characterize more complex motion such as this. Figure 12 shows raw measurement locations and circular fits for each orbital radius. The change in radius and relative change in the orbital plane position that is required to balance the centripetal and gravitational forces is clearly visible.

FUTURE WORK

Toward dynamic laser tracker calibration

Our results demonstrate the ability to accurately characterize the 3D dynamics of a moving object using a laser tracker while the laser tracker remains in a stationary measurement mode. This suggests a technical roadmap for the full 3D characterization and calibration of a laser tracker under dynamic conditions. This can be envisioned in the following scenario: A moving calibration target would be measured with the laser tracker in a stationary mode via the aliasing technique described above. The laser tracker would then be using in a dynamic mode where it follows the same moving calibration target so that a range of motion variables (position, velocity, etc.) are exercised in three dimension. Errors between the two measurements would then be quantified and parametrized based on these movement variables, thus giving the dynamic performance of just the laser tracker. As opposed to other methods[4] our proposed technique does not rely on the accuracy of reference geometries and motion stages being better than the laser tracker, and can directly characterize the dynamics of the test fixture and laser tracker independently. Other methods also require the laser tracker to lock onto an SMR probe fixed to the reference target. There are no such limitations in our technique on needing to lock to an SMR because the physical target is directly measured. This allows the dynamics of the reference target to be measured independently from the dynamics of whatever laser tracker and probe combination are used, such as a laser line scanner or touch probe.

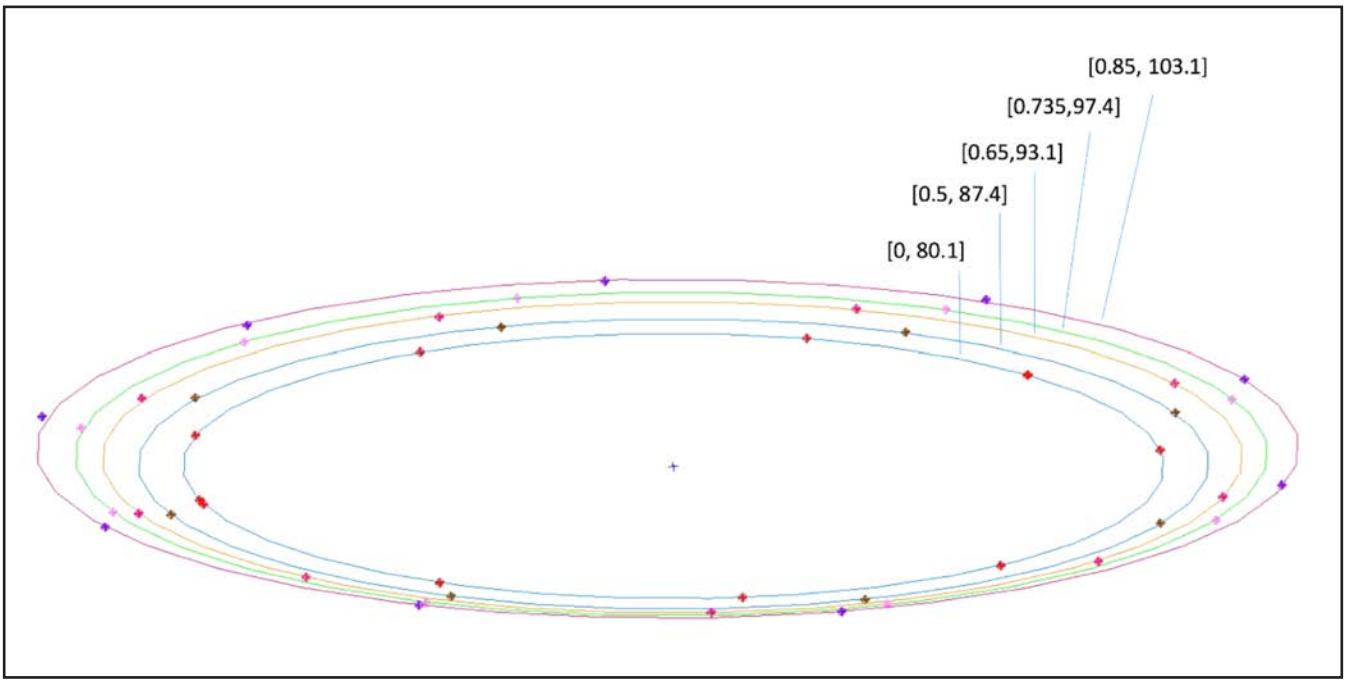

Figure 12. Orbital radii for each rotation frequency: data points and fitted radii are shown, and the bracketed values are in units [frequency (Hz), radius (mm)]; the banking of the orbital path due to the change in orbital radii and orbital plane is clearly visible

CONCLUSION

In this article we present a technique for performing dynamic measurements using a laser tracker where the laser tracker can remain in a stationary mode. The use of digital cameras in the Pixel Probe provides a means for decoupling the dynamics of a laser tracker from the dynamics of the object under measure. This is achieved by adjusting the frame rate of the cameras so that a moving object appears stationary to the Pixel Probe and therefore to the laser tracker. The object can then be measured with the laser tracker in a stationary mode even though the object is moving. Furthermore, because the dynamics of an object can be determined independent from the dynamics of the laser tracker, this technique may provide a way to generally characterize and calibrate the dynamic performance of a laser tracker without the need for special fixtures or precision test geometries. Measurements of rotating rigid optical targets using this technique are compared to the case where these targets remain stationary. Errors between the rotating and stationary cases are shown to be within the uncertainty of the laser tracker, thereby validating this technique. Measurements of a constantly rotating mass suspended from a string are also presented which demonstrate the ability to characterize a dynamically changing object in 3D using this technique. The motion of the mass based on these measurements is compared to Newton's equations of motion for an object under continuous rotation. The rotation frequency of the mass is able to be determined from purely spatial measurements obtained using this technique. Several rotation frequencies are measured and compared to the known rotation frequency. On average agreement in frequency data is shown to be better than 1 percent.

ACKNOWLEDGEMENTS

The authors would like to offer special thanks to William A. Hoff, Ph.D., of the Department of Electrical Engineering and Compuer Science at the Colorado School of Mines for his discussions and input rearding machine vision.

REFERENCES

[1] Gordon, J.A., Novotny, D.R., and Curtin, A.E., "A Single Pixel Touchless Laser Tracker Probe," *The Journal of the CMSC*, Vol. 10, No. 2, pp. 12–21, 2015.

[2] Gaskill, J., *Linear Systems, Fourier Transforms, and Optics,* John Wiley and Sons, 1978.

[3] Halliday, D. and Resnick, R., *Fundamentals of Physics, Third Edition*, pp. 111, John Wiley and Sons, 1988.

[4] Morse, E., and Welty, V., "Dynamic Testing of Laser Trackers," *CIRP Annals—Manufacturing Technology*, No. 64, pp. 475–478, 2015.